Oak Ridge National Laboratory

Interaction of runaway electrons with whistler and Alfvén waves in the presence of impurity injection

D. A. Spong, C. Paz-Soldan, W.W. Heidbrink, D. del-Castillo-Negrete, M. Beidler, C. Lau, X.D. Du, A. Lvovskiy, K.E. Thome, M.A. Van Zeeland, L. Baylor

7th Annual Theory and Simulation of Disruptions Workshop

Princeton Plasma Physics Laboratory

August 5 - 7, 2019

U.S. DEPARTMENT OF ENERGY

Acknowledgements

Research sponsored by the Laboratory Directed Research and Development Pro- gram of Oak Ridge National Laboratory, managed by UT-Battelle, LLC, for the U. S. Department of Energy and by U.S. Department of Energy, Office of Science Contract No. DE-AC05-00OR2

Runaway mitigation issues

- SPI (shattered pellet injection) is the primary runaway dissipation method approved for ITER
  - Successful on DIII-D, to be tested on JET in September
- Both runaway generation and dissipation can drive instabilities via $\partial f_{runaway}/\partial E > 0$, anisotropy
  - Whistler waves
  - Alfvén waves (shear/compressional)
  - Fan instability
- Modeling + experiments needed to understand which mechanisms are most active => ITER predictions
  - Collisions with screened impurities, neutrals, synchrotron/Bremsstrahlung radiation, wave particle interactions

Runaway control/modeling regimes include:

- **Formation: prediction of runaway source**
  - Disruption prediction/modeling
  - Runaway generation/acceleration
  - Collisional and synchrotron losses
  - Avalanche effects
- **Suppression/dissipation strategy**
  - Runaway interaction with SPI ablation cloud
  - Collisional effects, impurities, screening, synchrotron/Bremsstrahlung losses, etc.
  - Ohmic and inductive field acceleration
  - Interaction with electromagnetic waves, MHD, field line stochasticity
- **For this talk we focus on the dissipation phase**

Argon SPI into a RE Beam on DIII-D Shows Rapid Dissipation of the RE Current

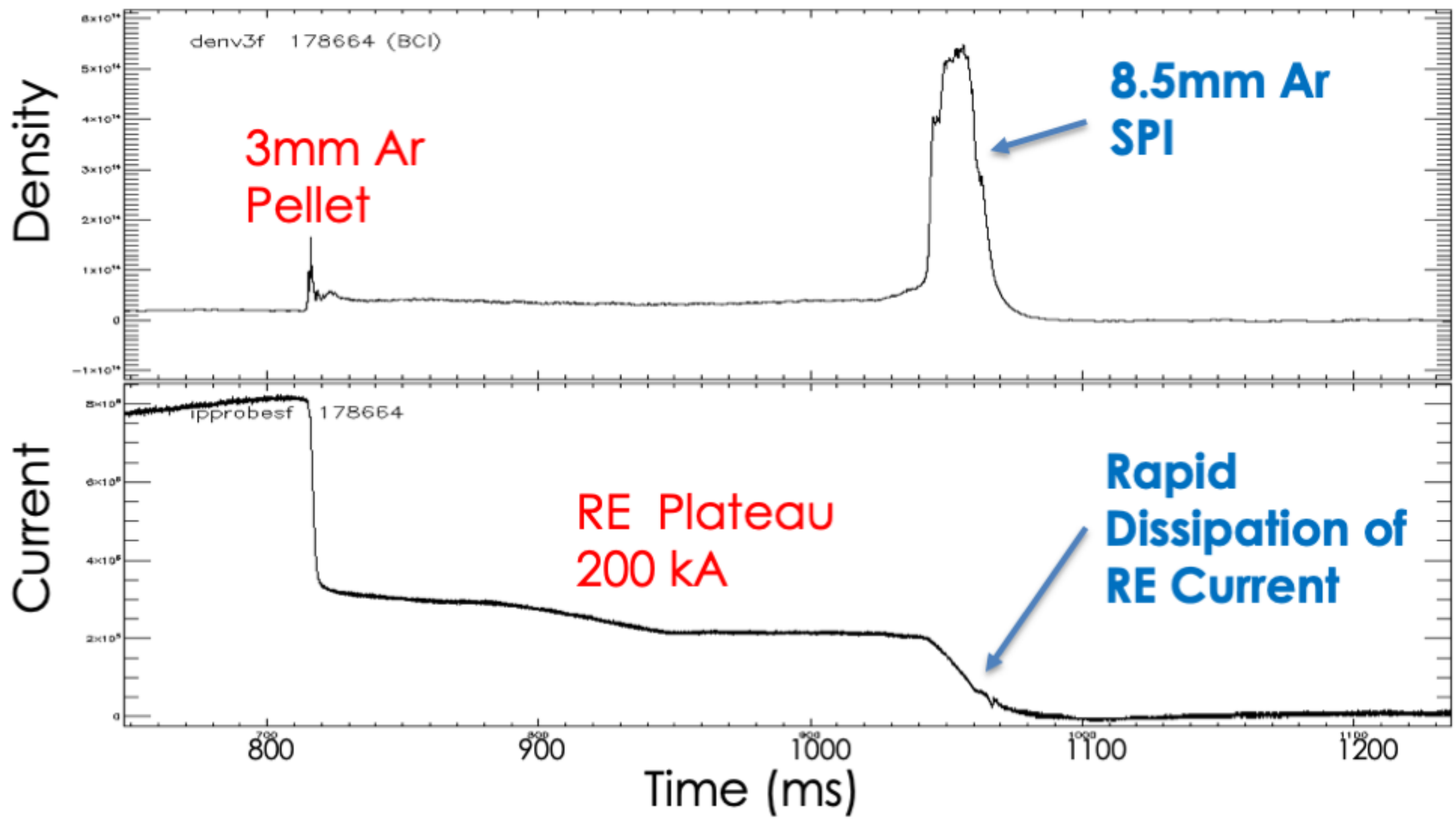

- Ar SPI has been used into a RE beam and shows the ability to collisionally dissipate the RE current on a 20 ms time scale.
- Physics question to answer is scaling the dissipation rate to ITER

Relativistic orbit trajectory models

Trajectory equations in Boozer Coordinates

[A. Cooper, et al., PPCF **39**, 931 (1997);
R. White, et al., PPPL-5078, 2014]

$$\dot{\theta} = \frac{eB^2\rho_\parallel}{m_0\gamma D}\left(\psi' - \rho_\parallel G'\right) + \frac{G}{\gamma D}\left(\frac{\mu}{e} + \frac{eB\rho_\parallel^2}{m_0}\right)\frac{\partial B}{\partial r}$$

$$\dot{\zeta} = \frac{eB^2\rho_\parallel}{m_0\gamma D}\left(\chi' - \rho_\parallel I'\right) - \frac{I}{\gamma D}\left(\frac{\mu}{e} + \frac{eB\rho_\parallel^2}{m_0}\right)\frac{\partial B}{\partial r}$$

$$\dot{r} = \frac{1}{\gamma D}\left(\frac{\mu}{e} + \frac{eB\rho_\parallel^2}{m_0}\right)\left(I\frac{\partial B}{\partial \zeta} - G\frac{\partial B}{\partial \theta}\right)$$

$$\dot{\rho}_\parallel = -\frac{1}{\gamma D}\left(\frac{\mu}{e} + \frac{eB\rho_\parallel^2}{m_0}\right)\left[\left(\chi' + \rho_\parallel I'\right)\frac{\partial B}{\partial \zeta} + \left(\psi' - \rho_\parallel G'\right)\frac{\partial B}{\partial \theta}\right]$$

$$\text{where}\quad D = G\chi' + I\psi' + \rho_\parallel\left(GI' - IG'\right) \qquad \rho_\parallel = \frac{\gamma m_0 \mathrm{v}_\parallel}{eB}$$

$$\psi = \text{poloidal flux}, \quad \chi = \text{toroidal flux}$$

$$\gamma = \left(1 - \mathrm{v}^2/\mathrm{c}^2\right)^{-1/2} \qquad \mu = m_0\gamma^2\mathrm{v}_\perp^2 / 2B$$

+ fluctuating field terms from R. White, et al., PPCF **52** (2010)

Non-canonical coordinates

outside closed flux surfaces and including magnetic islands
[J. Cary, A. Brizard, Rev. Mod. Phys. **81**, 693 (2009)]

$$\frac{d\mathbf{X}}{dt} = \frac{1}{\mathbf{b}\cdot\mathbf{B}^*}\left(q\mathbf{E}\times\mathbf{b} - p_\parallel\frac{\partial \mathbf{b}}{\partial t}\times\mathbf{b} + \frac{m\mu\mathbf{b}\times\nabla B + p_\parallel\mathbf{B}^*}{m\gamma_{gc}}\right)$$

$$\frac{dp_\parallel}{dt} = \frac{\mathbf{B}^*}{\mathbf{b}\cdot\mathbf{B}^*}\cdot\left(q\mathbf{E} - p_\parallel\frac{\partial \mathbf{b}}{\partial t} - \frac{\mu\nabla B}{\gamma_{gc}},\right)$$

where $\mathbf{B}^* = q\mathbf{B} + p_\parallel\nabla\times\mathbf{b}\,,$

$$\mu = \frac{\left|\mathbf{p} - p_\parallel\mathbf{b}\right|^2}{2mB} \qquad \gamma_{gc} = \sqrt{1 + \left(\frac{p_\parallel}{mc}\right)^2 + \frac{2muB}{mc^2}}$$

- This approach is developed in a KORCGC code by Matt Beidler
- Can readily include magnetic islands, flux surface breakup, stochasticity => initial current quench

Full Lorentz orbit model

- KORC developed by Leopoldo Carbajal, Diego del-Castillo-Negrete
- Applied to synchrotron radiation emission from runaways

Collision operator model

Collision operator of G. Papp, et al., Nuc. Fusion **51** (2011) 043004, App. B (merges together relativistic and non-relativistic limits for e-e scattering)

$$\lambda = \mathrm{v}_{\parallel}/\mathrm{v} \qquad \mathrm{q} = \gamma \frac{\mathrm{v}}{c} \qquad \gamma = \left(1 - \frac{\mathrm{v}^2}{c^2}\right)^{-1/2}$$

Monte Carlo collision operator:

$$\lambda_{new} = \lambda_{old}\left(1 - \nu_d \Delta t\right) \pm \left[\left(1 - \lambda_{old}^2\right)\nu_d \Delta t\right]^{1/2}$$

$$q_{new} = q_{old} + \nu_{E1}\left(q_{old}\right)\Delta t \pm \left[\nu_{E2}\left(q_{old}\right)\Delta t\right]^{1/2}$$

$$\nu_d = I = \frac{\sqrt{1+q^2}}{\tau q^3}\left[Z_{eff} + \phi(x_e) - G(x_e) + \frac{\varepsilon q^2}{1+q^2}\right]$$

$$\nu_{E1} = \frac{1}{\tau q^2}\left\{-J(q)\left(1+q^2\right) + \frac{\partial}{\partial q}\left[J(q)P(q)\right]\right\}; \quad \nu_{E2} = \frac{1}{\tau q^2} J(q)P(q)$$

$$J(q) = \frac{q^2}{\varepsilon\left(1+q^2\right)} G(x_e); \quad P(q) = \frac{\varepsilon\left(1+q^2\right)^{3/2}}{q}$$

$$\phi(x) = Error\ \ function = \frac{2}{\sqrt{\pi}}\int_0^x e^{-y^2}\,dy; \quad G(x) = \frac{1}{2x^2}\left[\phi(x) - x\phi'(x)\right]$$

$$\varepsilon = \frac{kT_e}{m_e c^2}; \quad x_e = \frac{q}{\sqrt{2\varepsilon\left(1+q^2\right)}}; \quad \tau = \frac{4\pi\varepsilon_0^2 m_e^2 c^3}{ne^4 \ln\Lambda}$$

OAK RIDGE National Laboratory

Collision operator + screened impurity effects

Collision operator of G. Papp, et al., Nuc. Fusion **51** (2011) 043004, App. B (merges together relativistic and non-relativistic limits for e-e scattering)

$$\lambda = \mathrm{v}_{\parallel}/\mathrm{v} \qquad q = \gamma\frac{\mathrm{v}}{c} \qquad \gamma = \left(1-\frac{\mathrm{v}^2}{c^2}\right)^{-1/2}$$

Monte Carlo collision operator:

$$\lambda_{new} = \lambda_{old}\left(1-\nu_d\Delta t\right) \pm \left[\left(1-\lambda_{old}^2\right)\nu_d\Delta t\right]^{1/2}$$

$$q_{new} = q_{old} + \nu_{E1}\left(q_{old}\right)\Delta t \pm \left[\nu_{E2}\left(q_{old}\right)\Delta t\right]^{1/2}$$

Impurity screening effects modify pitch-angle scattering

$$\nu_d = I = \boxed{\frac{\sqrt{1+q^2}}{\tau q^3}\left[Z_{eff}\right.} \left. + \phi(x_e) - G(x_e) + \frac{\varepsilon q^2}{1+q^2}\right]$$

Impurity screening effects modify slowing-down/drag

$$\nu_{E1} = \boxed{\frac{1}{\tau q^2}\left\{-J(q)\left(1+q^2\right) + \frac{\partial}{\partial q}\left[J(q)P(q)\right]\right\}}; \qquad \nu_{E2} = \frac{1}{\tau q^2}J(q)P(q)$$

L. Hesslow, O. Embréus, et al., PRL **118**, 255001 (2017).

$$J(q) = \frac{q^2}{\varepsilon\left(1+q^2\right)}G(x_e); \qquad P(q) = \frac{\varepsilon\left(1+q^2\right)^{3/2}}{q}$$

$$\phi(x) = Error\ \ function = \frac{2}{\sqrt{\pi}}\int_0^x e^{-y^2}\,dy; \quad G(x) = \frac{1}{2x^2}\left[\phi(x) - x\phi'(x)\right]$$

$$\varepsilon = \frac{kT_e}{m_e c^2}; \quad x_e = \frac{q}{\sqrt{2\varepsilon\left(1+q^2\right)}}; \quad \tau = \frac{4\pi\varepsilon_0^2 m_e^2 c^3}{ne^4\ln\Lambda}$$

OAK RIDGE National Laboratory

Modifications to collision frequencies for quantum/kinetic screening effects

- Fast electron colliding on bound electrons of partially ionized impurities
- Pitch angle scattering: elastic electron-ion collisions
  - Quantum Born approximation, density functional theory
- Energy scattering: inelastic electron-electron collisions
  - Bethe stopping power formula
- We use Hesslow model: equations (4) and (7)

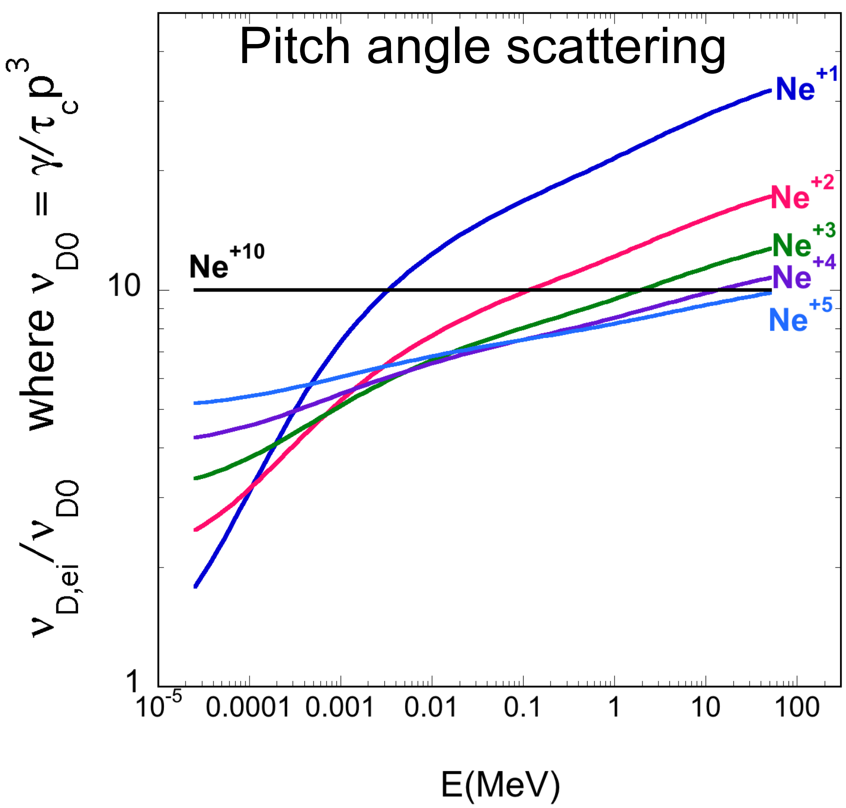

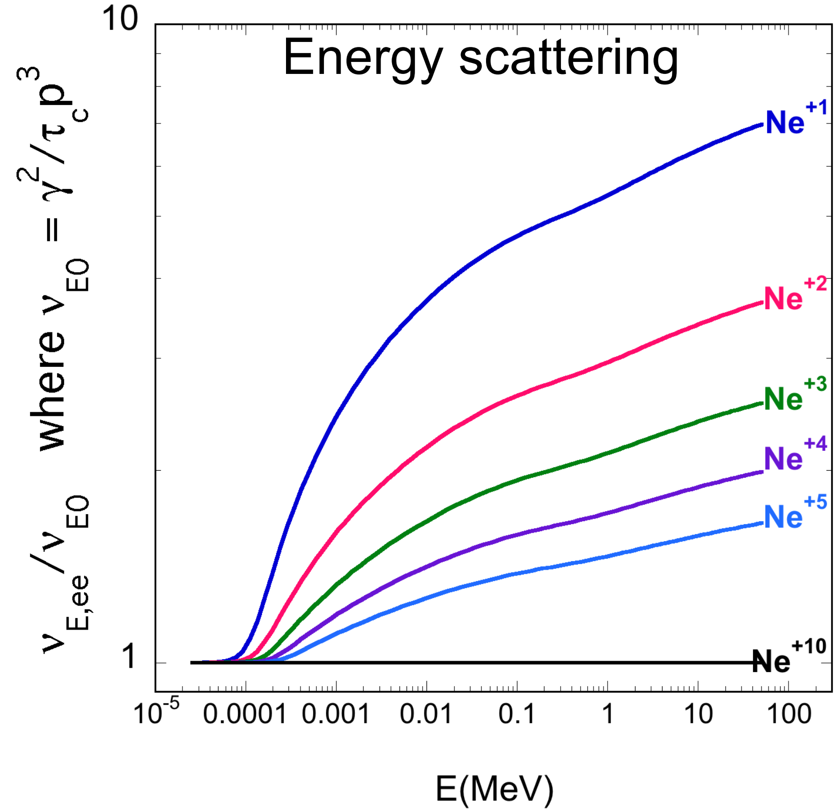

Synchrotron damping model includes momentum and pitch angle evolution

Synchrotron loss model [from G. Zhang and D. del-Castillo-Negrete, Physics of Plasmas 24, 092511 (2017)]

$$\frac{dp}{dt} = -\frac{\gamma p}{\tau_r}\left(1-\xi^2\right)$$

$$\frac{d\xi}{dt} = \frac{\xi\left(1-\xi^2\right)}{\tau_r \gamma}$$

where :

$$\xi = p_{\|} / p = \cos\theta, \quad \tau_r = 6\pi\varepsilon_0 m_e^3 c^3 / \left(e^4 B^2\right)$$

$$p \text{ is normalized to } m_e c \Rightarrow \gamma = \sqrt{1+p^2}$$

τ_r sets the time scale for synchrotron energy losses
Typically, τ_r is in the range of

- 1.3 seconds for DIII-D parameters
- 0.2 seconds for ITER parameters

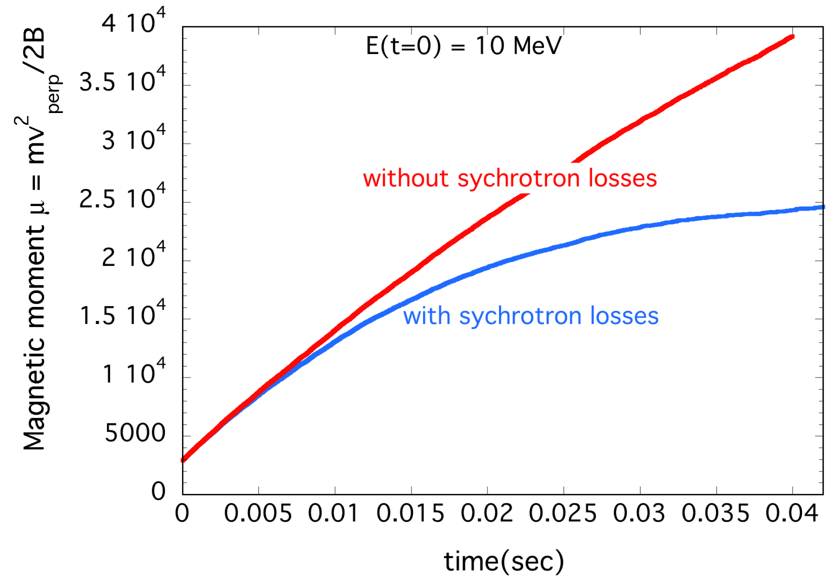

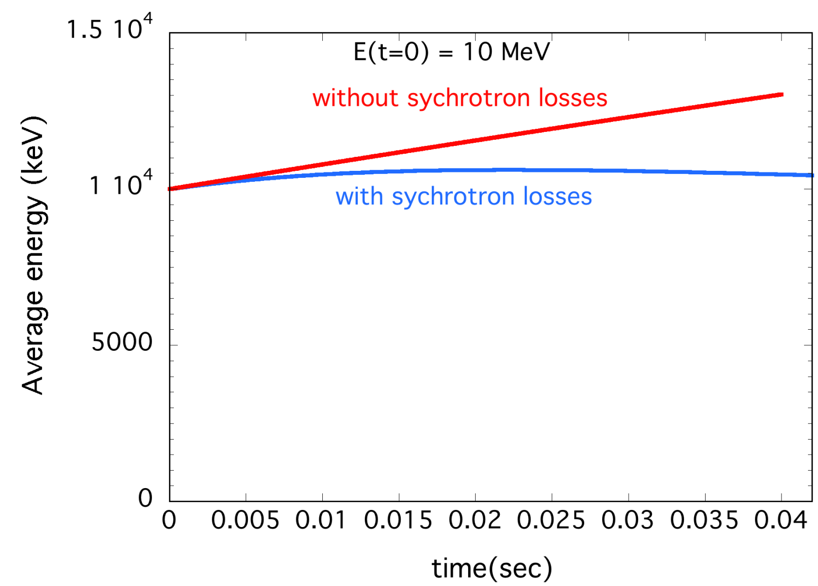

OAK RIDGE National Laboratory

Bremsstrahlung losses are included, but small for energies considered here

$$\left[\frac{d}{dt}(\gamma-1)m_e c^2\right]_{Bremsstralung} = -2\beta c N \kappa Z(Z+1)\frac{\alpha}{\pi}(\gamma-1)\left[\ln(2\gamma)-\frac{1}{3}\right]$$

where: $\kappa = 2\pi r_e^2 m_e c^2, \quad r_e = \dfrac{e^2}{4\pi\varepsilon_0 m_e c^2}, \quad \alpha = \dfrac{1}{137}$

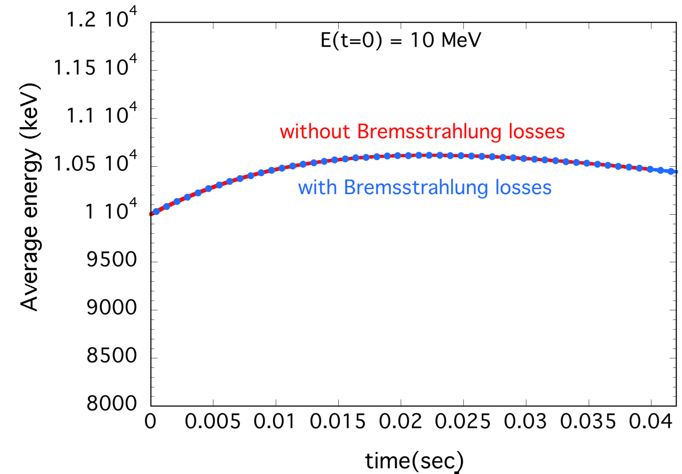

- Radiation from interaction between runaways and nuclear charge of heavy impurity
  - Based on M. Baktieri, et al., Phys. Rev. Lett. **94** (2005) 215003
- Derived from a radiative stopping power model
- More recent single particle binary collision models indicates this may be an overestimate
  - O. Embréus, A. Stahl, T. Fulop, New J. Phys. **18** (2016) 093023
- However, it does not play a significant role in the dissipation, this is not an issue for now.

Electric field model: acceleration/spatial variation

- Free-fall acceleration equation

$$\frac{d}{dt}\left(\gamma m_0 \vec{\mathrm{v}}\right) = -e\vec{E} = -e\frac{\partial \vec{A}}{\partial t}$$

- Ampere's law

J runaway
- Inferred from data
- Runaway generation rates
- Monte Carlo

$$\vec{\nabla}\times\vec{B} = \vec{\nabla}\times\vec{\nabla}\times\vec{A} = \mu_0\vec{J} = \mu_0\left(\vec{J}_{runaway} + \vec{J}_{plasma}\right)$$

- Runaway-dominated limit:

$$\frac{\partial}{\partial R}\frac{1}{R}\frac{\partial}{\partial R}(RA) + \frac{\partial^2 A}{\partial z^2} = \frac{\mu_0 n_{runaway} e^2}{m_0}\frac{A}{\sqrt{1+A^2}} = \frac{k^2 A}{\sqrt{1+A^2}} \quad \text{where} \quad k^2 = \frac{\omega_{pr}^2}{c^2} \quad \text{with} \quad \omega_{pr}^2 = \frac{n_{runaway} e^2}{m_0 \varepsilon_0}$$

electron skin depth parameter

$$A \equiv \frac{-e}{m_0 c}\left[A_\phi(\vec{r},t) - A_\phi(\vec{r},t=0)\right]$$

where

$$\frac{\mathrm{v}_\phi}{c} = \frac{A}{\sqrt{1+A^2}}$$

D. Spong, et al., Nuclear Fusion **14** (1974) 397

During pellet-induced runaway current ramp-down, runaways are accelerated both due to loop voltage and L dI/dt

$$Current = I_{runaway} = \pi a_r^2 n_{runaway} ec$$

$$\Rightarrow n_{runaway} = \frac{I_{runaway}}{\pi a_r^2 ec}$$

e.g., for estimated paramters of DIII-D

runaway dominated case: $I_{runaway} = 300kA,\ a_r = 25cm$

$$\Rightarrow n_{runaway} = 3.2\times 10^{10}\, cm^{-3}$$

$$c/\omega_{pe} \approx 3\ cm,\ ka_r = 8.4$$

Typical DIII-D Argon SPI pellet runaway suppression
ΔI = 200 kA, dI/dt ~ - 4 MA/sec

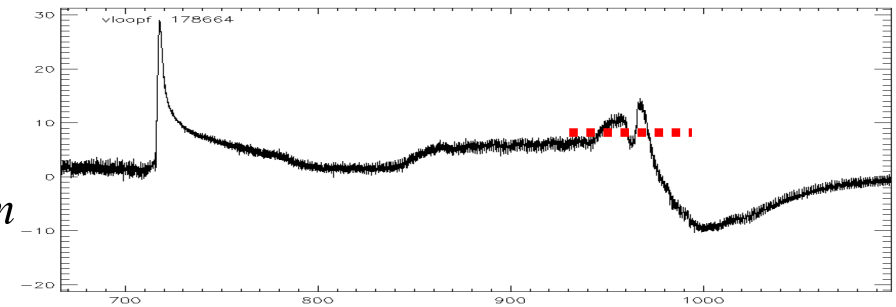

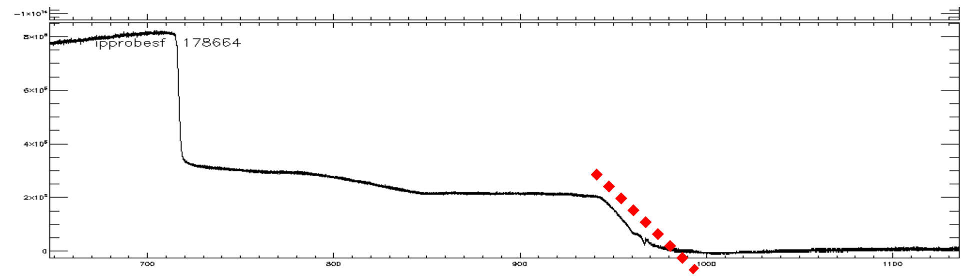

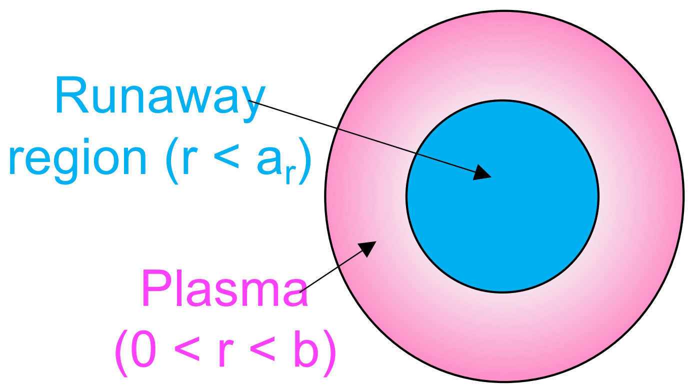

~0.5 v-sec ~0.3 v-sec

$$A(t)\big|_{r=a_r} = \frac{e}{2\pi R_0 m_0 c}\left\{\int_{t_0}^{t} \varepsilon_{loop}(t')dt' - \mu_0 R_0\left[I(t)-I(0)\right]\ln\frac{b}{a_r}\right\}$$

OAK RIDGE National Laboratory

Solving coupled nonlinear acceleration + Ampere's equation indicates:

- Early time acceleration is highly non-uniform
- Runaway current profile fills in with time
- Runaway beam has nonlinear resistivity
- For mildly-relativistic energies => runaways highly conductive => skin effect
- For relativistic energies => no further current increase => weak skin effect

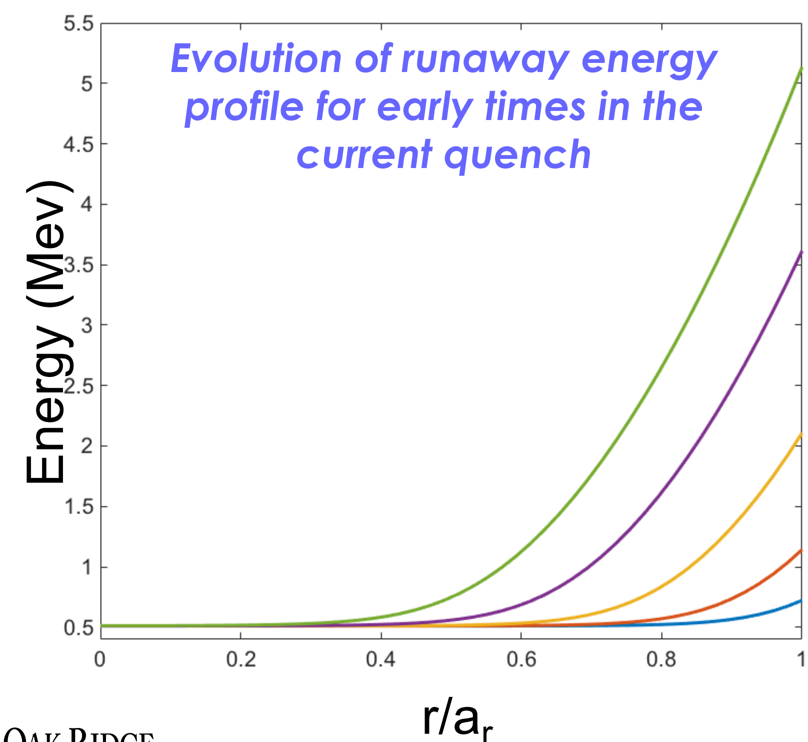

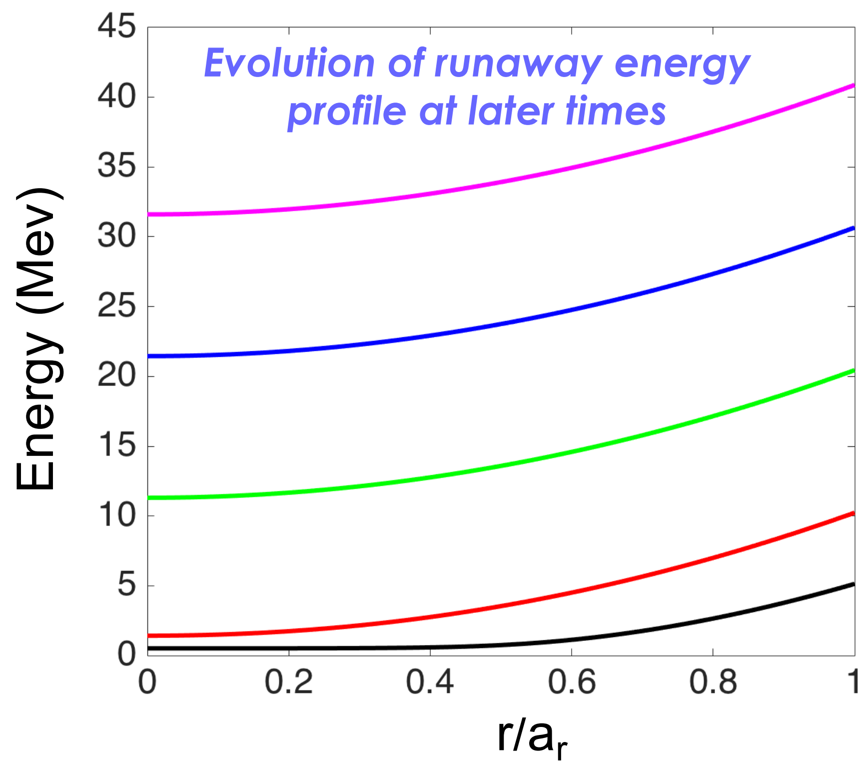

Electric field acceleration (loop voltage + inductive component) modifies runaway dissipation rates

- For this example (E_0 = 10 MeV, $n_{Ar+1} = 2 \times 10^{14}$ cm^{-3}), the runaway energy decrease from collisions is approximately balanced by electric field
- The runaway current is sustained longer, but eventually drops as pitch angle scattering accumulates

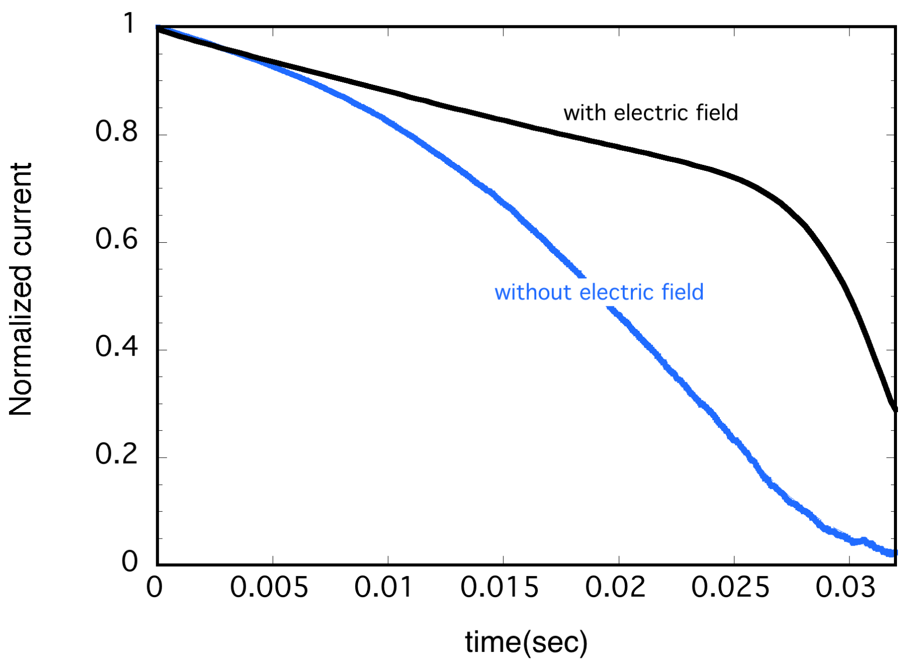

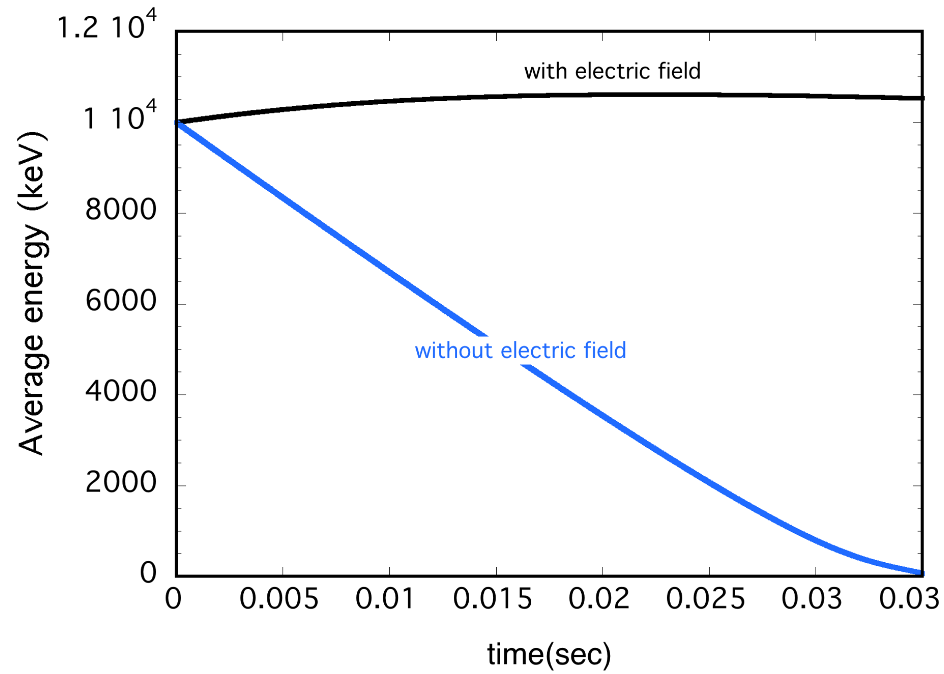

OAK RIDGE National Laboratory

Monte Carlo simulation of SPI runaway dissipation on DIII-D

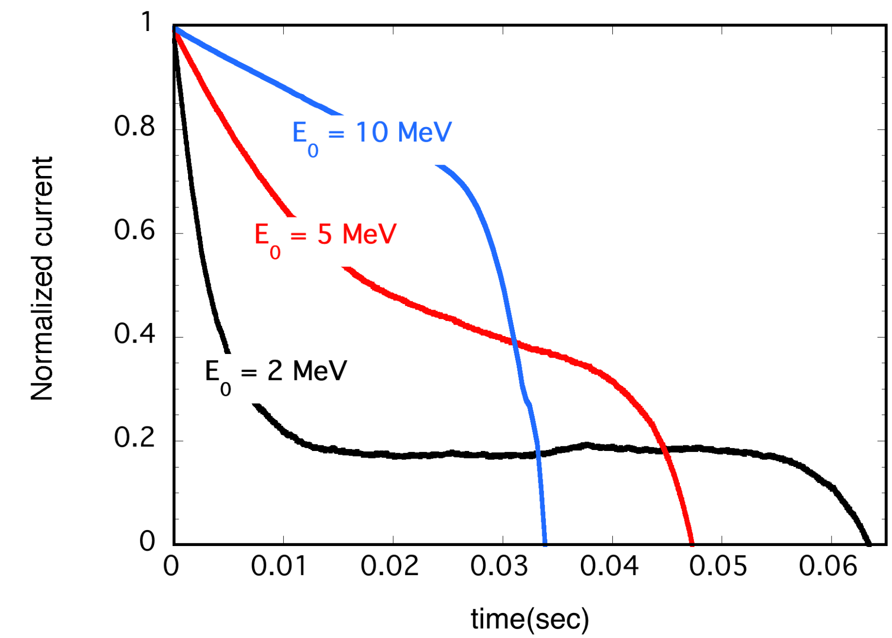

- Fixed density profile => next step: time-dependent profile
- Electric field with loop + inductive components
- Singly ionized Argon
- Bremsstrahlung + synchrotron radiation

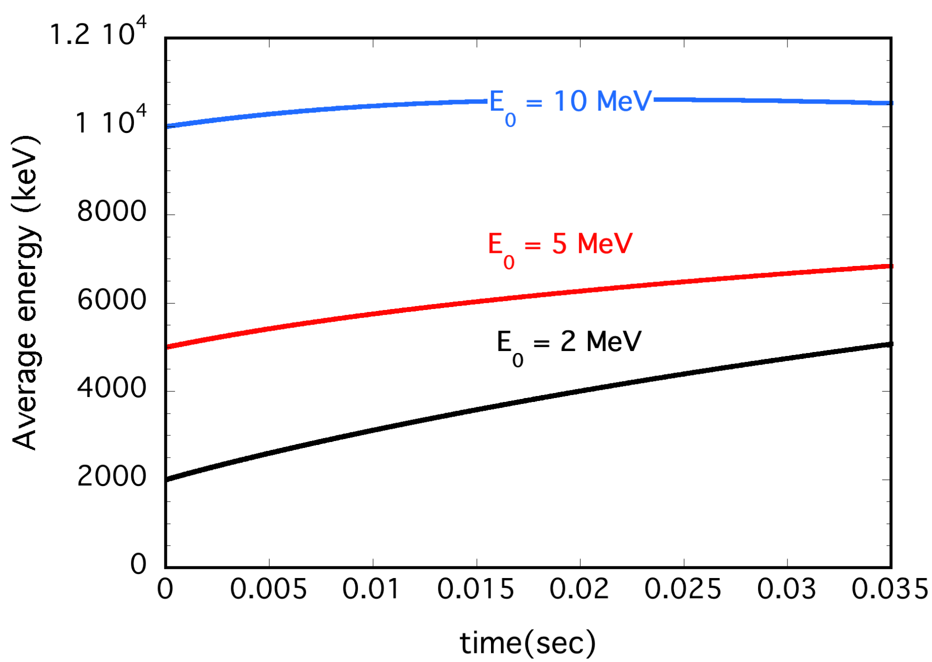

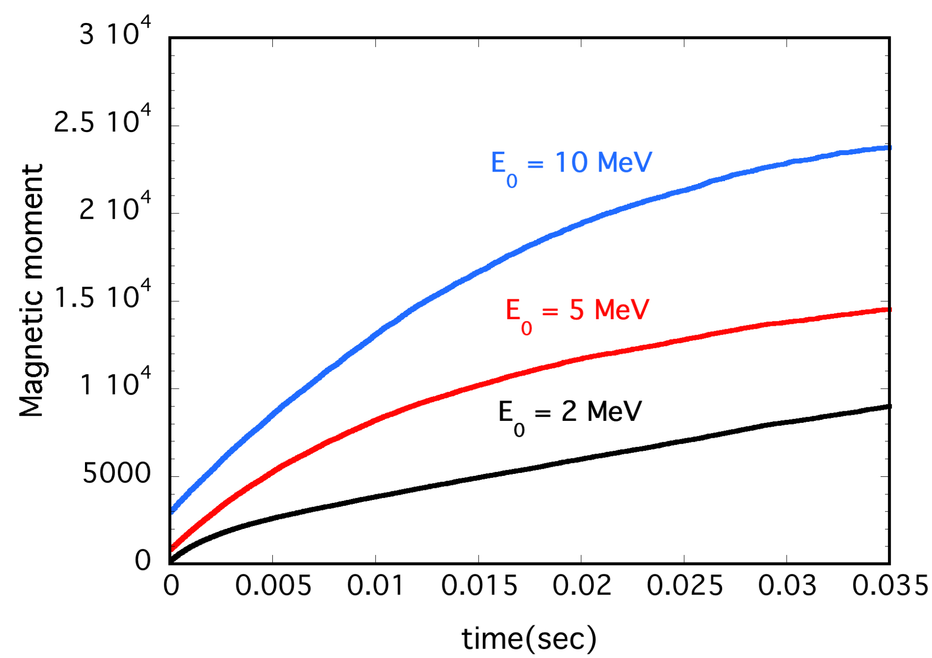

Within expected parameter ranges, collisional Monte Carlo dissipation rates are in the same range as experiments (30 – 40 msec), further improvements needed:

- Pellet ablation cloud model – evolution in space and time
- Runaway-neutral collisions
- Time-dependent equilibria
- Multiple ion components
- Runaway beam pinch effect (E_{ϕ} x B_{pol} drifts)
  – D. Spong, et al. Nuclear Fusion **14** (1974) 507.
- **But, need to look for anomalies between classical collisional models and experimental decay rates**
  – Both runaway acceleration and deceleration are expected to create conditions for instability drive
  – Positive velocity gradients, strong spatial gradients, anisotropy
  – Runaway generation anomalies
    - Experimental runaway generation rates deviate from predictions (R. Granetz, et al. POP (2014)
    - Related to effects from whistler instabilities - C. Liu, et al., PRL (2018)

Runaway interactions with waves

- Whistler instabilities
  - Coupling through resonances (Anomalous Doppler, Cherenkov), drive from anisotropy, radial gradients, non-monotonic f(E)
- Alfvén instabilities (shear, compressional Alfvén)
  - Driven by anisotropy, radial gradients, non-monotonic f(E)
  - Can be non-resonant and still cause scattering
  - Scattering effects accumulate from long residence of runaways in presence of wave
- MHD instabilities
  - Islands, chaotic field lines, 3D fields
- Whistler/Alfvén activity was topic of recent DIII-D Frontier Science experiment
  - Connections to ionospheric/solar/astro-physics

Whistler measurements utilized DIII-D's Ion Cyclotron Emission (ICE) diagnostic*

- **Whistlers observed on fast wave antenna straps & toroidal RF loops**
  - Not observed on density interferometer
- **Measurements in the 100 to 200 MHz frequency range**

Antenna

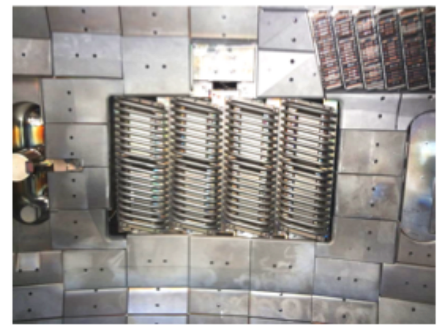

RF Loop

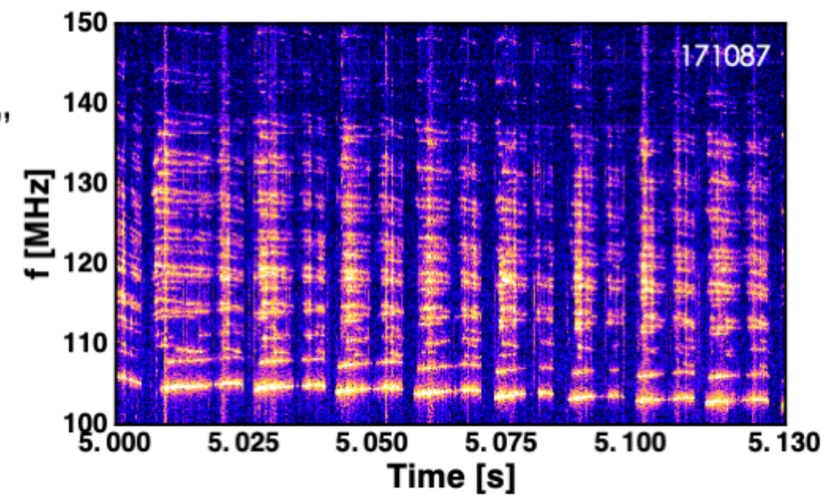

*K.E. Thome, "Ion Cyclotron Emission on the DIII-D tokamak," 15th IAEA Technical Meeting on Energetic Particles in Magnetic Confinement Systems (2017)

D. Spong, W. Heidbrink, C. Paz-Soldan, et al., Phys. Rev. Lett. **120** (2018) 155002.

DIII-D NATIONAL FUSION FACILITY

DIII-D low density Quiescent Runaway Electron regime provides a controllable runaway component for whistler wave physics studies

- **Decreasing plasma density leads to increasing runaway generation**
  - Controlled by gas puff
- **Verified by rising hard x-ray signals**
- **RF amplitudes in the 100 – 200 MHz frequency range related to whistlers**

C. Paz-Soldan, et al., PRL **118** (2017)

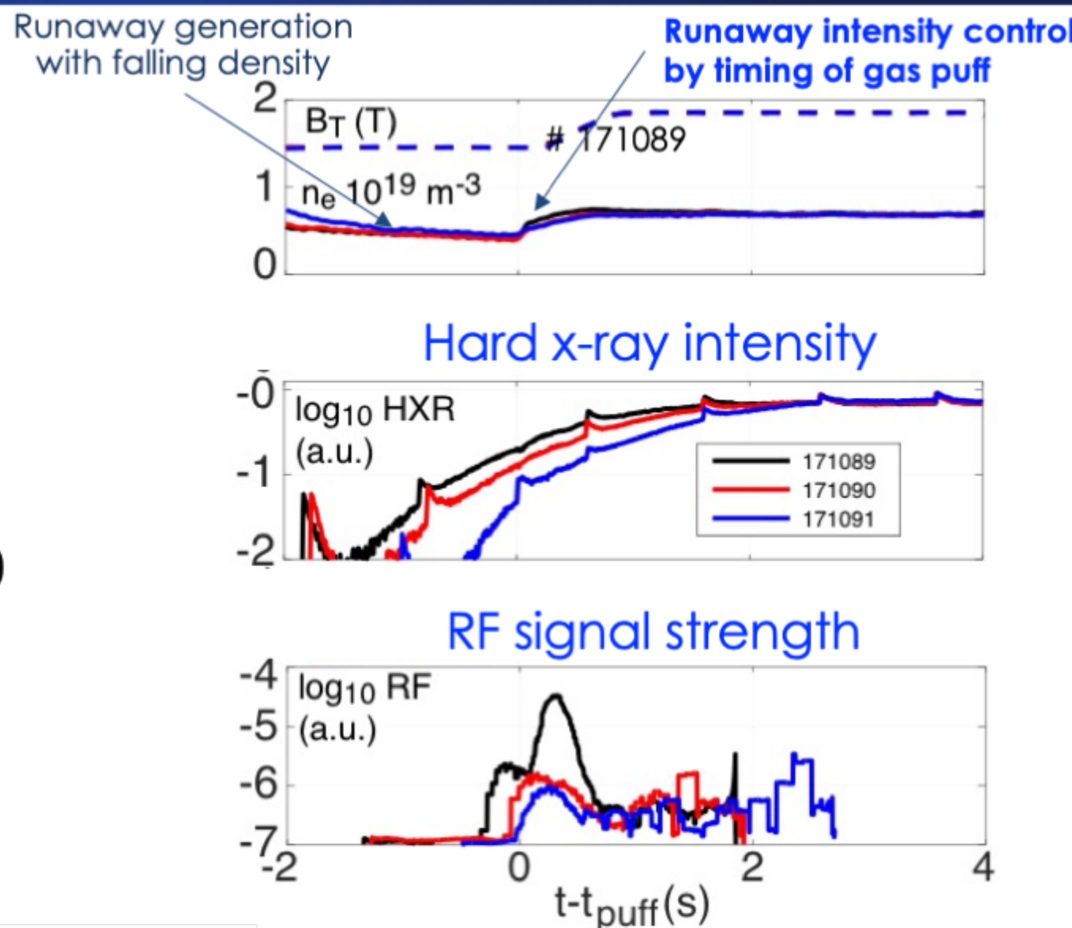

Both anomalous Doppler and Cherenkov resonances can be active (depends on $k_{\parallel}$)

- **Resonance:** $\omega - k_{\parallel} v_{\parallel} - k_{\perp} v_d - l\Omega_{ce}/\gamma = 0$
- **Anomalous Doppler resonance: l = -1**
  - $k_{\parallel} v_{\parallel}$ and Ω_{ce} compete, leading to frequencies in the 100's MHz range
- **Cherenkov resonance: l = 0**
  - MHz frequency range for $k_{\parallel} \sim 0.01\ to\ 0.05 \times k$
  - Higher frequency $\omega \sim \Omega_{ce}$ for larger $k_{\parallel}$

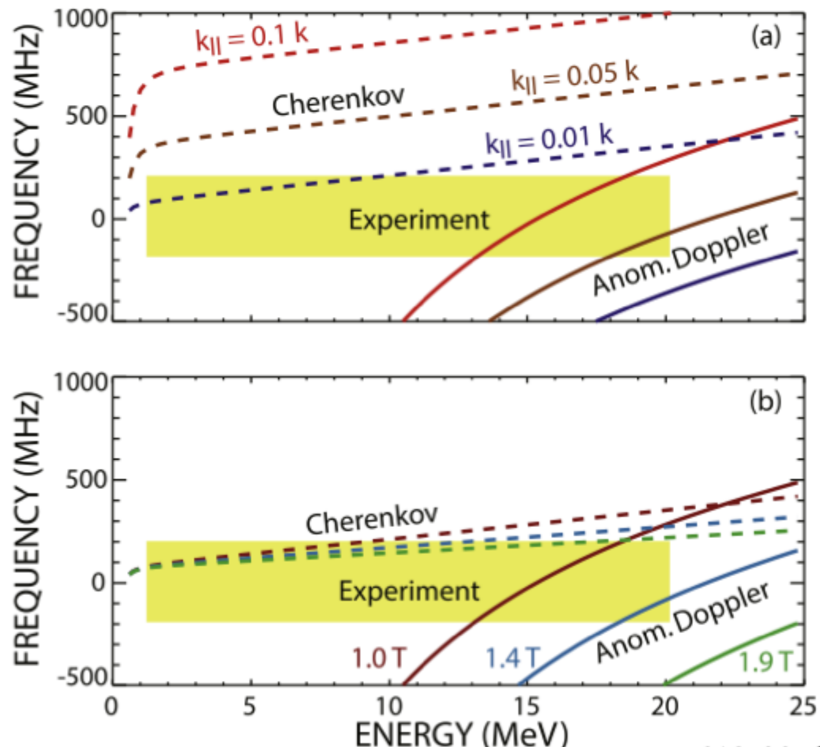

W. Heidbrink, et al., PPCF **61** (2019)

D. Spong, et al., DOE Frontier Science, Feb., 2019

Nonlinear dynamics show limit cycles that correlate whistlers with saw-teeth and ECE activity

- A range of phenomena observed both between discharges and within single discharges
- Whistlers disappear with sawtooth crashes
- Whistler cross-power often correlated with ECE
- At later times less correlation between whistlers/ECE/sawteeth
  - Evolving runaway gradients, velocity anisotropy, B field, scrape-off density

Sawtooth crashes: dashed vertical white lines

ECE: overlaid yellow curves

Integrated whistler power: white curves

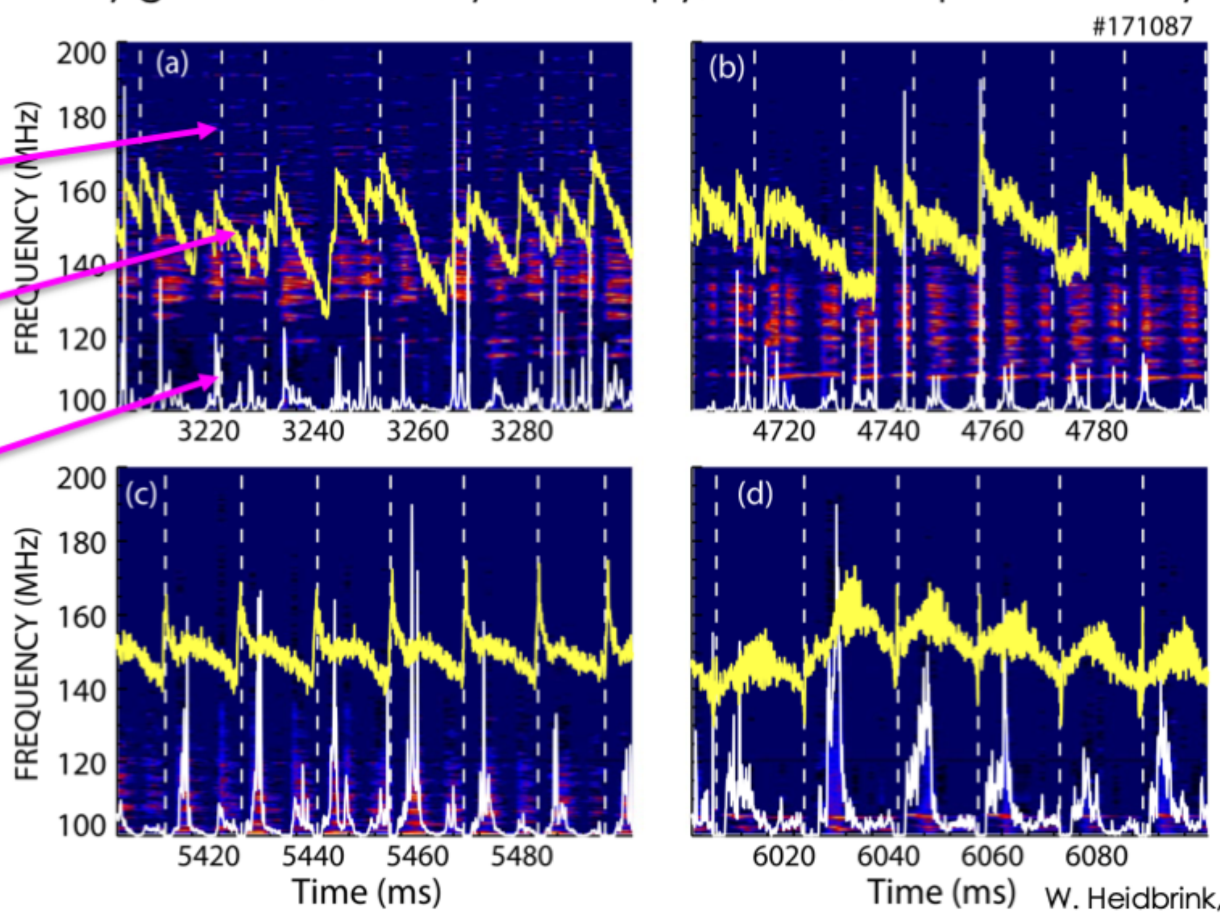

W. Heidbrink, et al., PPCF **61** (2019)

DIII-D NATIONAL FUSION FACILITY

Theoretical RF models also indicate irregular frequency peaks

- Future use in full orbit particle models
- Also used for launching external waves for runaway control

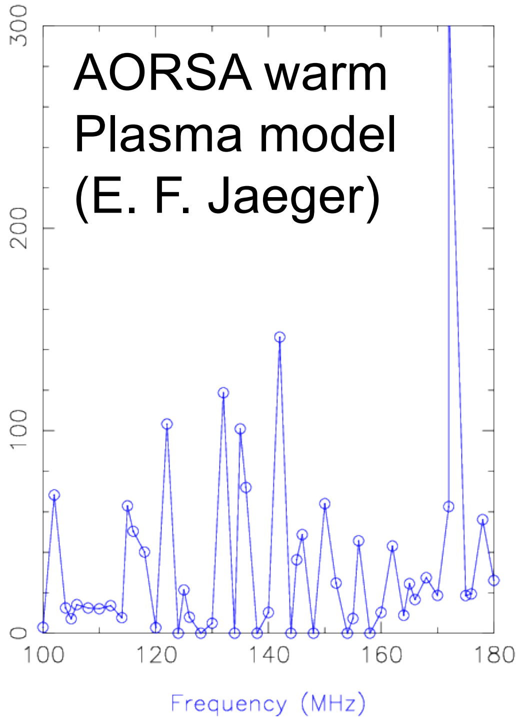

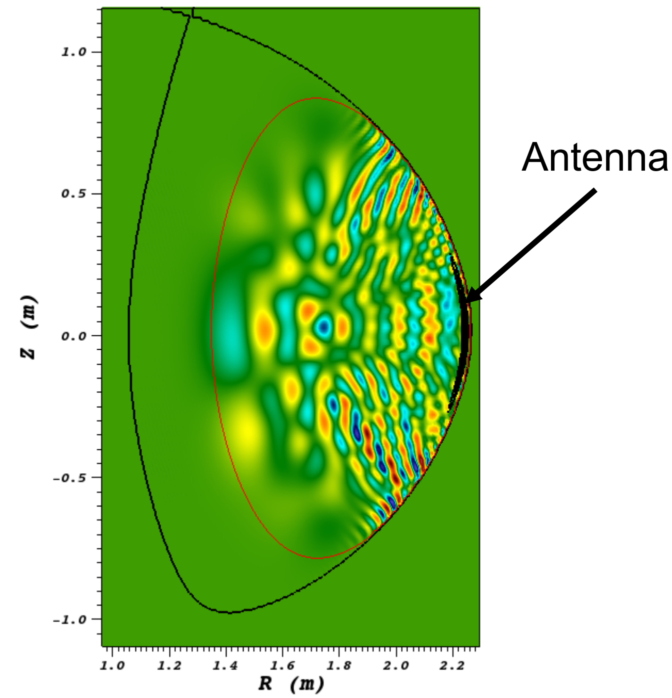

Simulated frequency spectrogram with increasing B

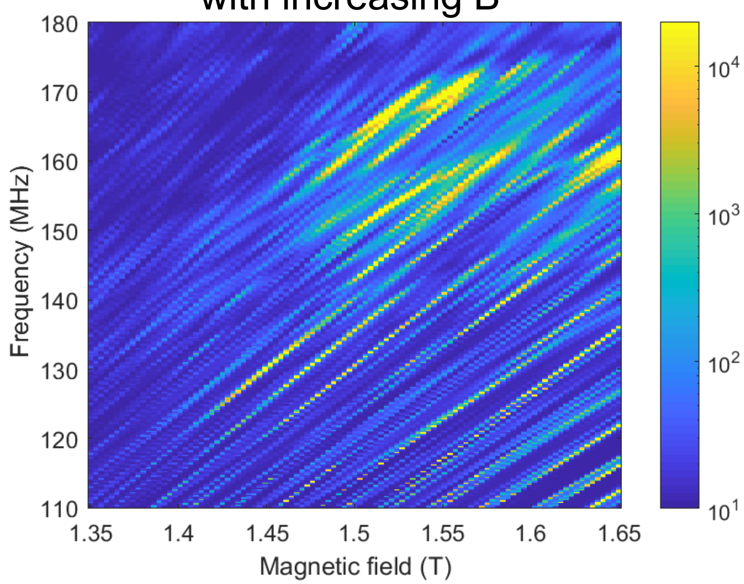

COMSOL cold plasma model (Cornwall Lau)

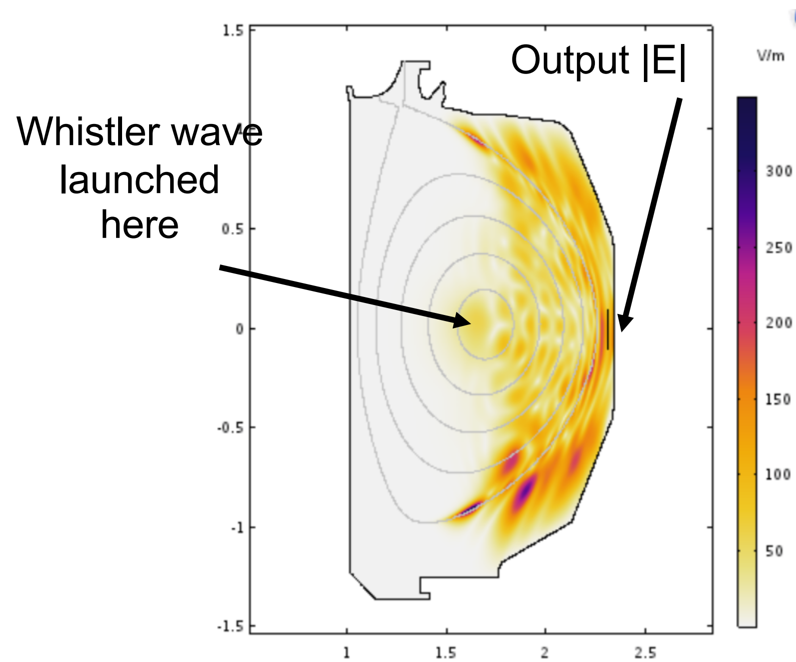

Alfvén instabilities and runaway electrons

- Alfvén waves generally present in all tokamak regimes
  - Shear Alfvén waves – HL-2A, Yi Ling, et al., IAEA-EX/9-3 (2016)
  - Compressional Alfvén waves – DIII-D, Andrey Lvovskiy, et al. (2019)
- Can be excited by beams/ICRF/hot electrons/alpha particles, or direct destabilization by runaways
- ITER: alphas can survive thermal collapse and drive AE's (?)

Alfvén modes predicted by FAR3D model for DIII-D runaway discharge

TAE/BAE modes in discharges 165124, 165139

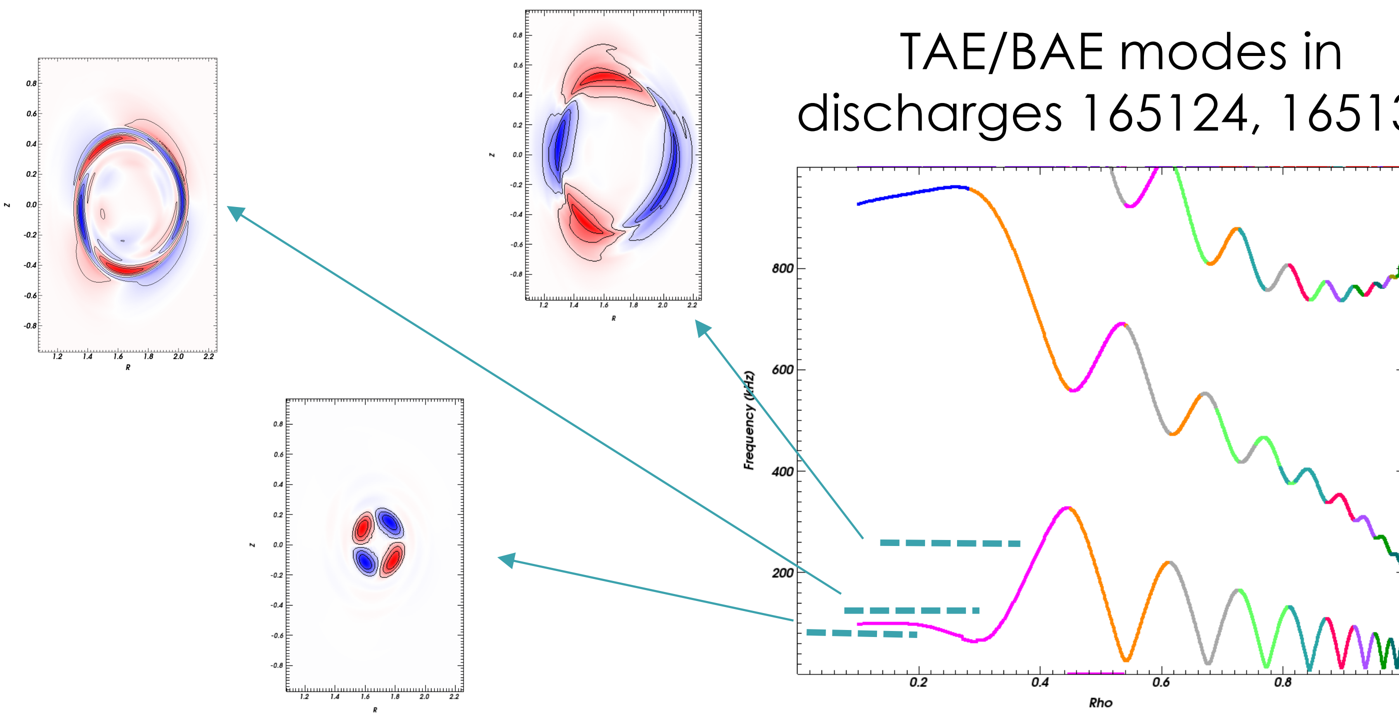

OAK RIDGE National Laboratory

Simulations of runaway dissipation with shear Alfvén instabilities show effects of scattering

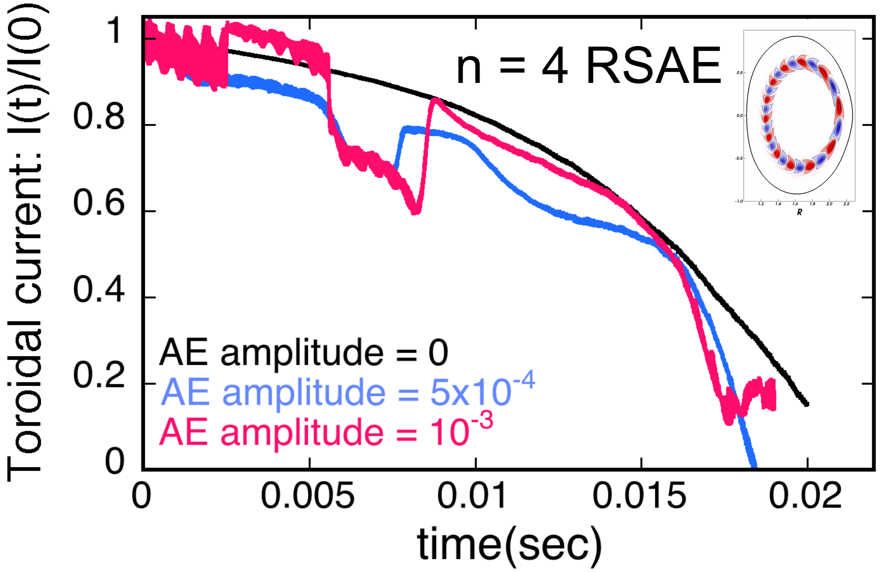

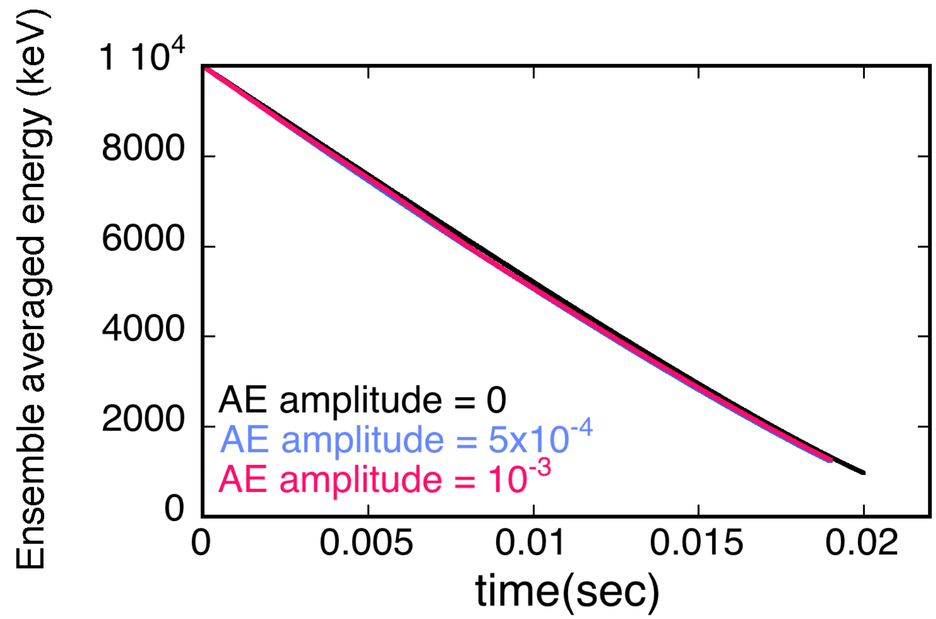

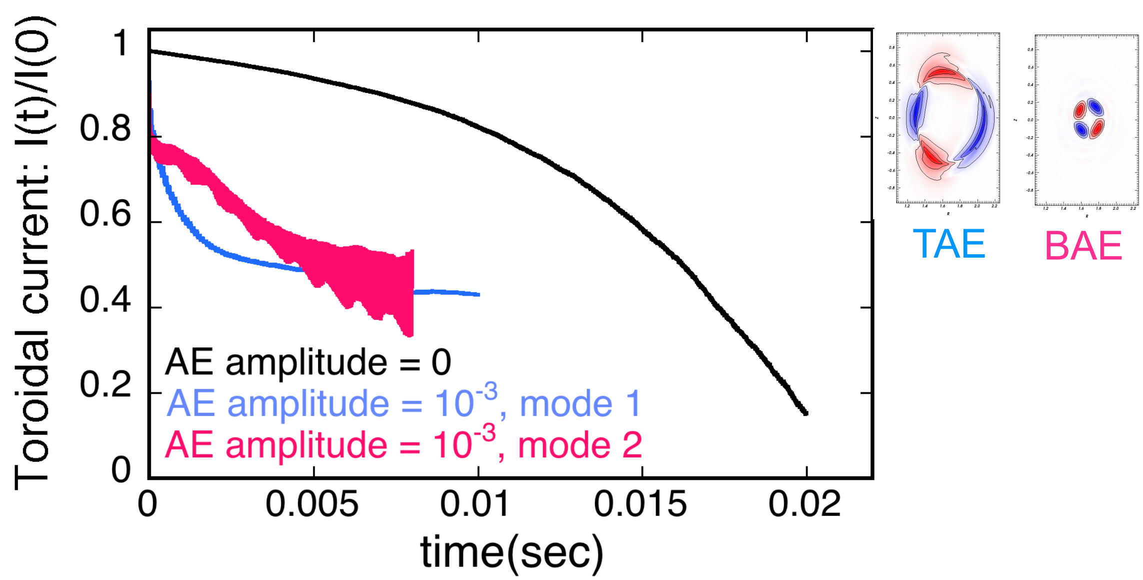

OAK RIDGE National Laboratory

Two Types of Runaway Electron Beam Instabilities Were Observed at Large Positive and Negative Loop Voltage (U_L)

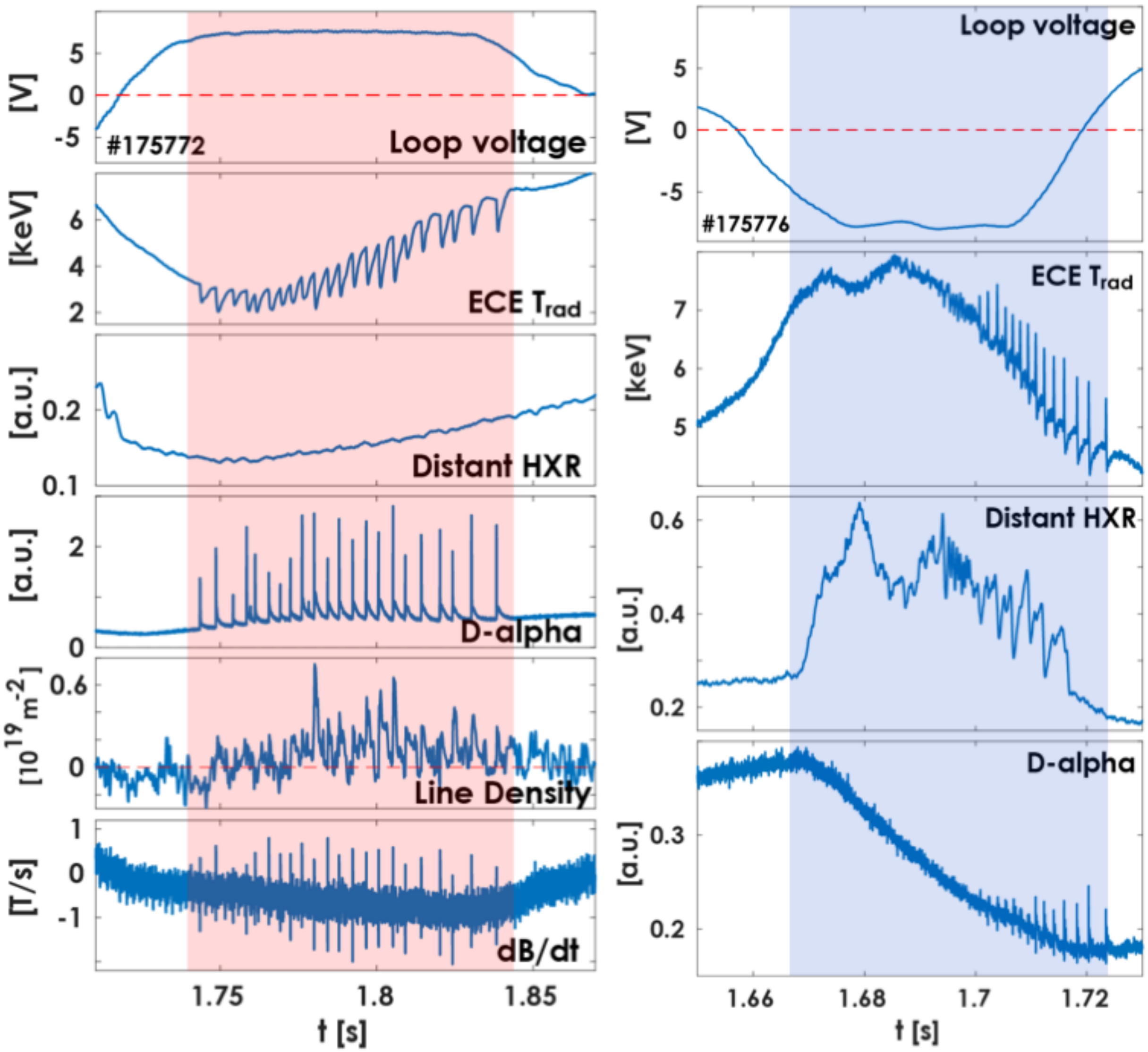

- **270 kA post-disruption runaway electron beam is produced after Ar killer pellet injection**
- **Ar is purged from the plasma by D_2 puff to reduce collisionality**
- **Rapid drops of ECE signals are observed when $U_L>0$**
  - **They correlate with bursts of Dα, density and dB/dt**
- **Strong increase of RE loss (fluct. of HXR signal) is observed when $U_L<0$**
  - **This correlates with bursts of ECE and Dα signals at the late stage**

DIII-D NATIONAL FUSION FACILITY

A. Lvovskiy/January 2019

D. Spong, et al., DOE Frontier Science, Feb., 2019

RE Loss at Large Negative Loop Voltage Correlates with Fast Fluctuations of Toroidal Magnetic Field

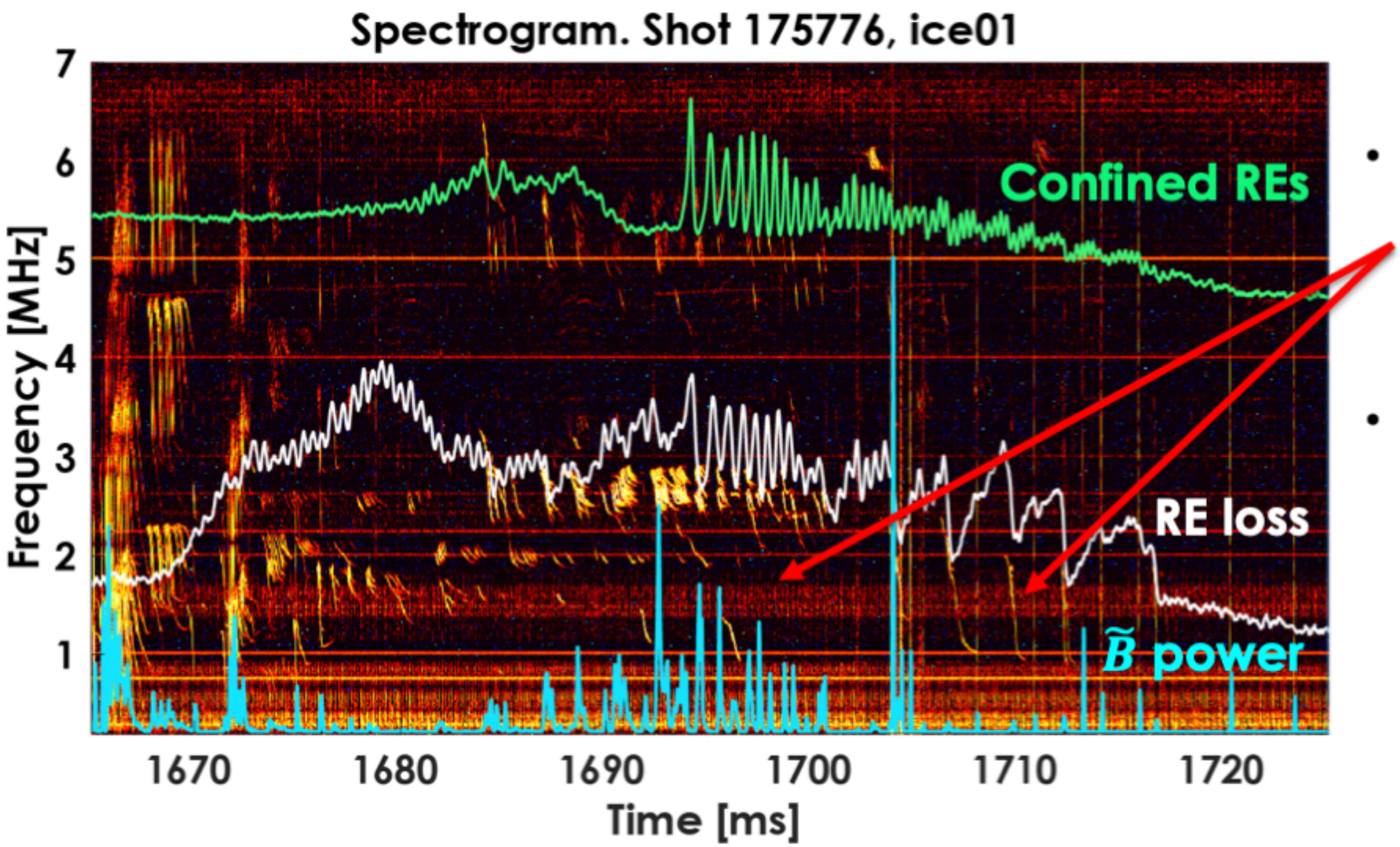

- HXR oscillations are well-correlated with oscillations of fast magnetic signals
- Fast magnetic signals strongly chirp and lie in the range 1-7 MHz

The Possible Instability at Large Negative Loop Voltage is Compressional Alfvén Wave

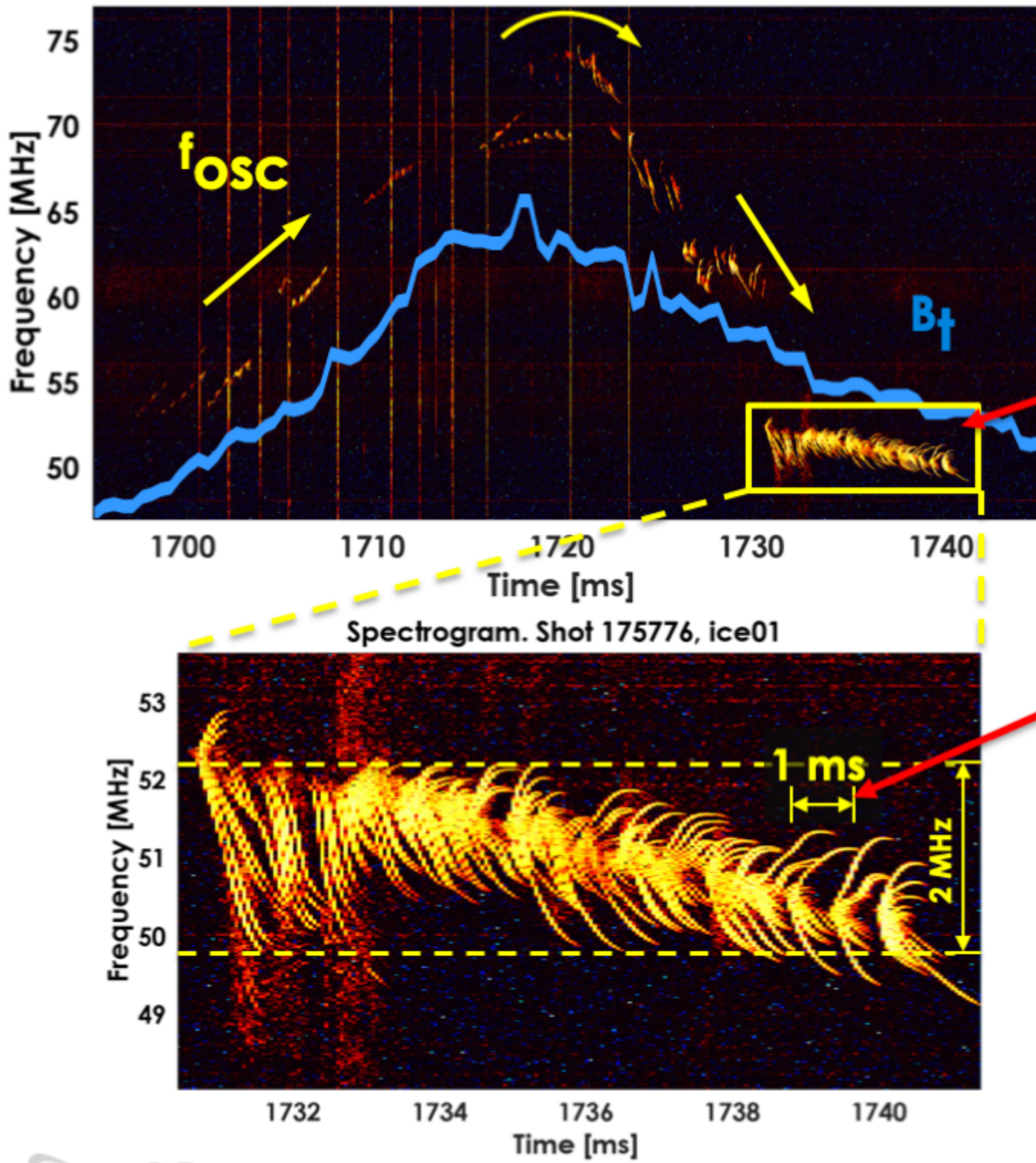

- There is high-freq. band of fast magnetic signals lying in the range 50-75 MHz
- It clearly shows the freq. dependence on B_{tor} caused by radial movement of RE beam: $\omega \propto v_A \propto B_{tor}$
- Sweeping modes are similar to GAEs and TAEs observed on many machines at much lower frequency (100 kHz → 50 MHz)
- The modes are supposedly CAEs driven by REs and upshifted due to low density $\omega \propto v_A \propto n_e^{-1/2}$
- **Observed instability is likely formation of non-monotonic RE tail → excitation of CAEs → fast pitch-angle scattering of REs → increased RE loss**

D. Spong, et al., DOE Frontier Science, Feb., 2019

Conclusions

- Monte Carlo modeling of runaway electron dissipation by shattered pellets demonstrated
  - Shielded impurity collisions + synchrotron/Bremsstrahlung radiation losses + electric field acceleration
  - Shattered pellet injection causes current decay
  - Modeling shows similar decay rate as DIII-D pellet experiments
  - Partially stripped impurity component can have a strong runaway dissipation effect
- Wave effects and runaways => can increase losses and provide new control methods
  - Alfvén modes can cause non-resonant cumulative scattering
    - Experimental evidence of both compressional and shear Alfvén effects
  - Whistler modes observed in DIII-D Frontier Science expt.
    - Scatter medium energy runaways
    - Correlated with runaway intensity
    - Discrete frequency bands in the 100 – 200 kHz range